



Importance of palladium dispersion in Pd/Al₂O₃ catalysts for complete oxidation of humid low-methane–air mixtures

Beata Stasinska^{a,*}, Andrzej Machocki^a, Katarzyna Antoniak^a, Marek Rotko^a, Jose L. Figueiredo^b, Filomena Gonçalves^b

^a University of Maria Curie-Skłodowska, Faculty of Chemistry, Department of Chemical Technology, Lublin, Poland

^b University of Porto, Faculty of Engineering, Laboratory of Catalysis and Materials, Porto, Portugal

ARTICLE INFO

Keywords:

Coal mine ventilation air
Utilization of methane
Catalytic oxidation of methane
Palladium catalysts
Water poisoning

ABSTRACT

The catalytic oxidation is considered as an environmental benign method for utilization of various methane-poor gas mixtures, including humid post-ventilation air of coal mines. The small crystallites of palladium phase in the Pd/Al₂O₃ catalyst decrease temperatures necessary to ignite the methane oxidation reaction and to achieve complete conversion of methane. The isotopic exchange of oxygen between the catalyst and the gas phase, the temperature-programmed reduction (TPR) with methane and the X-ray photoelectron spectroscopy studies suggest that it can result from a higher number of the Pd–PdO sites present on the catalysts with small palladium crystallites. The inhibiting effect of water vapour present in the reaction mixture increases with lower dispersion of palladium phase as well as with the water concentration in the feed. The larger palladium crystallites are more significantly affected by the presence of water. It is suggested that water vapour blocks the Pd–PdO active sites. The catalysts with small crystallites (<6.6 nm) of palladium can be successfully used for mitigation of the emission of methane from coal mine post-ventilation air and, after increasing of the methane concentration to 1–2 vol.%, for its utilization for the energy production. In the case of such catalysts even a high concentration of water vapour has the least negative influence on the catalyst activity and it will not interfere with obtaining of the 100% conversion of methane below 650 °C.

© 2008 Published by Elsevier B.V.

1. Introduction

Fugitive methane emitted from coal mines around the world, represents approximately 8% of the world's anthropogenic methane emissions that constitute 17% contribution to total anthropogenic greenhouse gas emissions. Poland is one of seven countries in the world with the largest amounts of methane emitted with ventilation air of coal mines [1]. Ventilation air is a difficult source of methane to use as an energy carrier, as air volume is large, methane is very diluted as well as variable in its concentration (0.1–1.0 vol.%) and flow rate. Until recently, there has been no technology that could be brought to mitigation of the emission of methane from coal mine post-ventilation air [1].

The catalytic oxidation of methane may be considered as a promising solution of methane-poor gas mixtures utilization. The process allows not only for complete oxidation of methane in its low-concentrated mixtures but it also may be carried out at moderate (depended on the catalyst used) temperatures. After mixing of post-ventilation air with methane recovered in the coal seam drainage systems (before mining and from worked areas of the mine) it is even possible to produce of energy.

Various catalysts were investigated in the oxidation of low-concentrated methane–air mixtures and the best performance of supported palladium catalysts was observed. The Pd/Al₂O₃ catalysts allow to initiate flameless combustion of methane from its low-concentrated air mixtures at the temperature lower than 300 °C and to achieve its total oxidation at temperatures at which no oxidation of nitrogen to nitrogen oxide occurs. Very good reviews on the catalytic complete oxidation of methane may be found in [2–6]. Palladium oxide is generally believed to be more active in methane oxidation than metallic palladium. However, it is also known that Pd co-existing with PdO increases the activity of palladium-based catalysts—palladium oxide supported on metallic palladium is more active than PdO dispersed directly on the oxide

* Corresponding author at: University of Maria Curie-Skłodowska, Faculty of Chemistry, Department of Chemical Technology, Maria Curie-Skłodowska SQ. 3, 20-031 Lublin, Poland. Tel.: +48 81 537 55 74; fax: +48 81 537 55 65.

E-mail addresses: stasinska@poczta.umcs.lublin.pl, beata.stasinska@interia.pl (B. Stasinska).

(e.g. Al_2O_3 , ZrO_2) support [2–7]. The pre-reduced and then re-oxidized (in the reaction mixture during oxidation of methane) palladium catalysts were much more active than unreduced catalysts [2–8]. It was suggested that the increase in the activity is based on the reconstruction and on decrease in the size of palladium oxide crystallites [2,5,6]. The Pd–PdO boundaries and $\text{Pd}^{2+}\text{O}^{2-}$ ion pairs are among surface peculiar sites considered as active centres in the methane oxidation reaction [2–6,9–12].

The application of the catalytic oxidation for the utilization of methane from coal mine ventilation air requires an acceptable activity of the catalyst even in the case of a high concentration of water vapour in the reaction mixture. The humidity of post-ventilation air is high. On the other hand, water vapour is also one of the methane oxidation products and it influences the activity of bottom layers (or inside of monolith channels) of the catalyst.

It was previously reported [2–6,13–32] that water vapour inhibits significantly the activity of palladium-based catalysts in the continuously performed oxidation of methane. The dependence of the reaction order was negative, from -0.25 up to -1.3 (most often -1) [3,9,13,17–19]. It was found that water is adsorbed or even it reacts reversibly with PdO to form adsorbed hydroxyls or palladium(II) hydroxide [2,3,13,20]. Some papers proposed that they effectively block of methane access to the palladium active phase [9,13,14] or that they are dehydrated only with the loss of oxygen [2,11]. The breaking of the OH bond in the hydroxide as the rate-limiting step for methane oxidation [2,14,21], the competition between methane and water for the active sites [3,17,23] or blocking of the re-oxidation of the catalyst from the gas phase [2] were also suggested. Usually, the poisoning effect was reversible—the activity of the catalysts more or less slowly (depending on the reaction temperature) returned to the level characteristic for the dry reaction mixture after removing of water from the feed and desorption of water from the surface [2–4,14,20,24,25] or after increasing in the reaction temperature [3,26]. However, in some pulsed studies the inhibitory effect of water was seen for even very long time in a dry gas environment [2,19,27]. Under continuously performed experiments water poisoning may be very strong even at high temperatures (up to 600°C) due to readsorption of water [27]. It should be also pointed out that water poisoning of palladium catalysts is still not fully understood [2].

As water vapour in the feed was increased the inhibition was more evident [3–5,9,14,18,28]. The inhibitory effect of water vapour was stronger at lower temperatures of the methane oxidation reaction [3,14,20,28]. The influence of water on the palladium-based catalyst activity was also affected by the nature of the support [2–4,14,19,29–31]. The higher hydrophobicity of the supports decreased inhibition caused by the adsorption of water vapour on the surface of the catalysts [19,30,31] but in the case of gamma-alumina supports the poisoning was very strong and unrecoverable [2,22,32]. The water poisoning was suppressed by addition of platinum to the palladium catalyst [4,22,24].

According to our up-to-date knowledge, the influence of water vapour on the activity of gamma-alumina supported palladium catalysts with variously dispersed palladium phase in the continuously performed oxidation of methane has not been studied yet.

The aims of the presented paper were (i) to characterize alumina-supported palladium catalysts with various dispersion of palladium active phase, prepared with a chlorine-free precursor, with a very similar palladium loading and with the same support and (ii) to examine how the presence of various concentrations of water vapour (including its high concentrations) in a low-methane–air mixture (resembled coal mine post-ventilation air enriched in methane from seam drainage systems, simulated water vapour concentrations expected at various points of the

length of the catalyst layer and inside of its pores) influences the activity of such catalysts. In contrast to many other papers, the different palladium dispersion in our paper was not achieved by sintering of catalysts, after which usually the texture of the support (total surface area, porosity) changeover also took place, or by variation of palladium contents. Our catalysts also do not contain chloride ions affecting the catalyst activity. Therefore, we were able to observe the role of the palladium phase dispersion in the inhibiting of its activity by water vapour, which was not interfered with different surface area and porosity of the catalyst support. They were the same in the case of all our catalysts. The changes in the catalyst activity caused by water vapour will be related only to different dispersion of the palladium phase.

2. Experimental

The commercial Al_2O_3 (Engelhard Al-0104) was used as the catalysts support. Palladium was deposited on the support by its double impregnation, at first with an EDTA solution and then with an aqueous solution of palladium nitrate $\text{Pd}(\text{NO}_3)_2$ [33]. The precursors were dried at 115°C , calcined at 500°C in air. In spite of large amounts of oxygen in coal mine post-ventilation air the catalysts were pre-reduced with hydrogen at 600°C for 2 h, prior to their use. Of course, a large excess of oxygen in the feed will oxidize some amounts of the metallic palladium [2–6,13,34,35]. However, it is well established that such pre-treatment enhances the activity of palladium catalysts in the complete oxidation of methane [2–8].

All Pd/ Al_2O_3 catalysts used had very similar palladium loading 0.30–0.38 wt%, equal porosity and the total surface area ($39\text{ m}^2/\text{g}_{\text{cat}}$). The double impregnation method, due to varied conditions (impregnation time, concentration of palladium solution) of the catalysts preparation enabled us to obtain catalysts with varied dispersion of palladium phase—from 4.6 to 13 nm. More details on the catalysts preparation and their basic properties are given in the reports [34,35].

The palladium content in the catalyst was determined by the X-ray fluorescence (XRF) method. The measurements were performed by the energy-dispersive XRF spectrometer (Canberra 1510) equipped with the liquid nitrogen-cooled Si(Li) detector. The AXIL software package was used for spectral deconvolution and for the calculation of palladium content.

The total surface area of the palladium catalyst was determined by using the BET method, as a result of argon adsorption on the catalyst surface at liquid nitrogen (77 K) temperature, assuming that argon atom occupies the surface of 0.157 nm^2 . The measurements were carried out in the ASAP 2405 N v1.0 analyser (Micromeritics).

The preliminary temperature-programmed experiments indicated that palladium oxide was reduced with hydrogen at a little above room temperature [34,35]. The decomposition of palladium hydride was observed at 70°C . At the temperature of 110°C palladium hydride was completely decomposed. Because of those findings hydrogen chemisorption was measured at 110°C , in the Autosorb-1-C analyser (Quantachrome). The temperature of 100°C was applied in [13] and the temperatures above 102°C for measurements of hydrogen chemisorption on palladium were also recommend in [2]. The mean size of palladium crystallites ($d_{\text{Pd}} = 1.12/D_{\text{Pd}}$; D_{Pd} is palladium dispersion) was calculated on the basis of the total hydrogen chemisorption ($\text{H}:\text{Pd} = 1:1$) under equilibrium pressure of 13.3 kPa.

The mean size of palladium crystallites was also measured by transmission electron microscopy (TEM)—LEO 906 operated at 120 eV. Prior to the TEM analysis the catalysts were reduced at 600°C for 2 h, cooled down up to 200°C under flowing H_2 and then

in He. The samples for microscopic measurements were prepared by placing droplets of a suspension of the catalyst in ethanol onto a standard Cu grid covered by a thin Formvar layer; then evaporating off the solvent in air at room temperature.

XPS analyses of reduced catalysts (the same procedure of the reduction as in the case of TEM measurements) were performed with the VG ESCALAB 200 A spectrometer using an unmonochromatized Mg K α radiation (1253.6 eV). The pressure in the analysis chamber was always $<1 \times 10^{-7}$ Pa. The charging effects were corrected using the C 1s level (285.0 eV) as reference. The XPS core level spectra were analysed with a fitting routine which decomposes each spectrum into individual, mixed Gaussian–Lorentzian peaks using a Shirley background subtraction over the energy range of the fit. The electron binding energies were calculated by reference to the energy of C 1s peak of contaminant carbon at 285 eV. The surface composition was calculated from the integrated peaks, using empirical cross-section factors for XPS (C 1s = 1, O 1s = 2.93, Al 2p = 0.54, Pd 3d(3d_{5/2} + 3d_{3/2}) = 16.04).

Temperature-programmed reduction of catalysts with methane was performed with the AMI-1 apparatus coupled with a quadrupole mass spectrometer HAL 201 RC (Hiden Analytical) using 0.4 g of catalyst placed in a flow quartz reactor with an internal diameter 7 mm. Prior to the TPR-CH₄ experiments, the catalyst samples were preliminary oxidized under 7% O₂/He flow from room temperature up to 480 °C, kept at this temperature for 10 min and then cooled under helium flow to room temperature. The end pre-treatment temperature was by 20 °C lower than the calcination temperature for all catalysts, so such pre-treatment did not change the characteristic of the catalysts. TPR-CH₄ measurements were carried out in the mixture of 10% CH₄/He, the linear temperature increase was 10 °C/min. CH₄ consumption and CO₂, CO, H₂ and H₂O evolution were monitored by mass spectrometer following the signal m/z = 15, 44, 28, 2 and 18, respectively.

The isotopic exchange of oxygen between the catalyst (0.2 g) and the gas phase was investigated after initial partial exchange of lattice oxide ions in catalyst with pulses (1 cm³) of labelled oxygen ¹⁸O₂ (Isotec, 99%) introduced into a helium stream (100 cm³/min.). The temperature was increased linearly (10 °C/min) up to 700 °C. Then, the catalyst was cooled under helium flow to room temperature. Afterwards, the catalyst was heated with a ramp of 20 °C/min in a stream of 10 vol.% ¹⁶O₂ in helium. The ¹⁶O₂, ¹⁶O¹⁸O and ¹⁸O₂ concentrations in the reactor effluent were monitored by the HAL 201 RC quadrupole mass spectrometer following the signal m/z = 32, 34 and 36, respectively.

The activity of the catalysts in the complete oxidation of methane was determined in a quartz reactor filled with the

catalyst (0.2 g, 0.75–1.2 mm) mixed with the pieces of quartz of 0.75–1.2 mm in diameter at the ratio of 1:10. The initial examination of the reaction of methane oxidation demonstrated that quartz showed very low catalytic activity only at temperatures (>650 °C) higher than those at which complete combustion of methane in the presence of catalysts was obtained. The reaction mixture composed of 2 vol.% of methane, 20 vol.% of oxygen, concentration of water vapour was changed from 0 to 20 vol.%, and the gas mixture was completed with nitrogen. Its space velocity was equal to 90,000 cm³/(g_{cat} × h). The water vapour was introduced into the reaction mixture by its saturation at various temperatures. The reaction temperature was increased step-by-step, until 100% methane conversion was achieved. The reaction product (carbon dioxide) and unreacted methane were analysed by on-line gas chromatography, using an Alltech CTR1 column made of two coaxial columns—the inner column was packed with a porous polymer mixture, whereas the outer one contained an activated molecular sieve packing.

3. Results and discussion

This paper presents how dispersion of palladium in alumina-supported catalysts, prepared with a chlorine-free precursor, with similar palladium loading, with the same Al₂O₃ support and the same total surface area and porosity, influences their properties in the complete oxidation of methane. Because of this, all possible differences in the activity and other catalyst properties may be related only to the different dispersion of palladium.

However, we had to prove the various dispersion of palladium. The transmission electron microscopy studies confirmed different dispersion of the palladium phase in the Pd/Al₂O₃ catalysts, previously [34,35] calculated on the basis of hydrogen chemisorption. However, as it is illustrated in Fig. 1, the transmission electron micrographs proved also some non-uniform distribution of palladium particle size. Thus, the technique of double impregnation applied for catalysts preparation consisted of two independent impregnation processes: (i) complexing of palladium ions with EDTA preliminary adsorbed on the alumina support surface and (ii) the support pores filling with an aqueous palladium nitrate solution. Only the former process lead to obtaining of controlled size of deposited crystallites of palladium active phase [33]. Nevertheless, the mean size of palladium crystallites determined with both methods (hydrogen chemisorption and transmission electron microscopy) was very similar. However, it should be also taken into account that the particle size can change during the reaction of methane oxidation [2]. In situ measurements are therefore desirable in further studies.

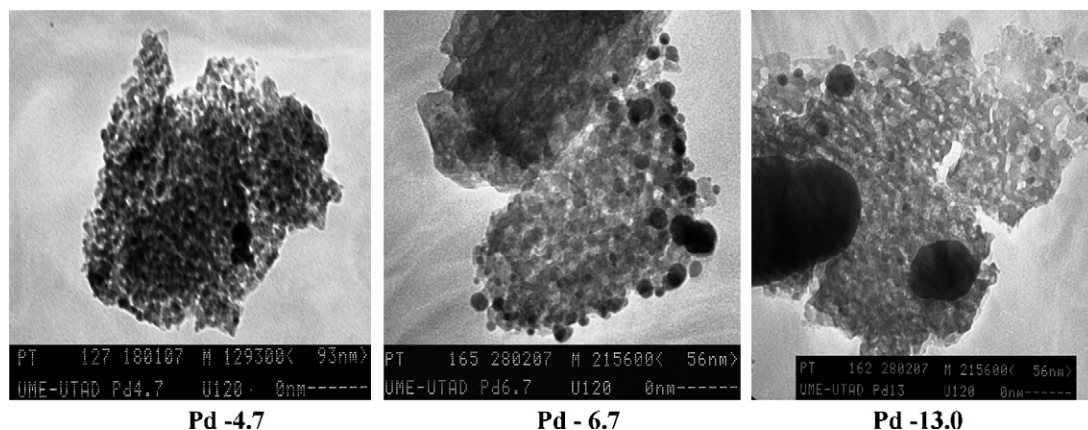


Fig. 1. Transmission electron microscopy images of reduced palladium catalysts.

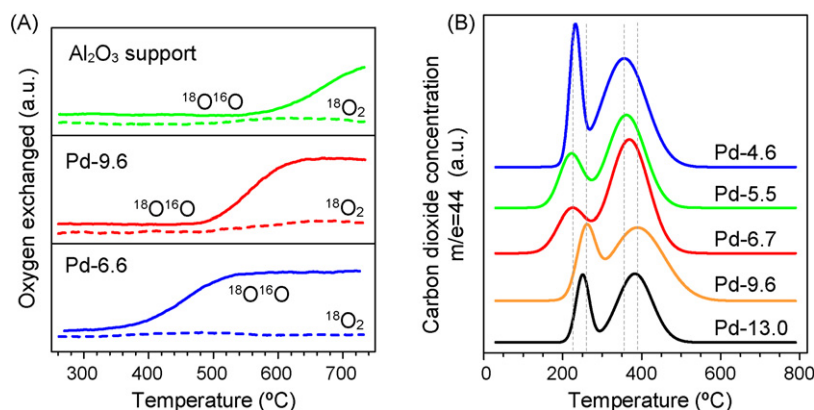


Fig. 2. Isotopic oxygen exchange in Pd/Al₂O₃ catalysts and Al₂O₃ support (A) and CO₂ evolution profiles obtained for the different Pd catalysts during the TPR-CH₄ experiments (B).

Fig. 2A shows that the exchange of oxygen isotopes from the gas phase with the catalysts took place at lower temperatures than in the case of pure alumina. The oxygen exchange in the higher-dispersed palladium catalyst occurred easier than in the catalyst with larger palladium crystallites. It can be interpreted that oxygen mobility is higher in the high-dispersed palladium catalysts, as well as it suggests that the higher amounts of lattice oxygen from small crystallites of the palladium phase may take part in the methane oxidation reaction. It was shown in [12] that a high oxygen exchange activity leads to high methane conversions. Additional support for above suggestions results from the TPR-CH₄ measurements.

Fig. 2B shows the profiles of CO₂ obtained in the TPR-CH₄ experiments. For the all catalysts reduction of palladium oxide-containing phase occurred in two steps, moved towards higher temperatures when the mean size of palladium crystallites was increased. The first step of carbon dioxide evolution, in the range 225–260 °C, is interpreted as the reduction of palladium oxide crystallites. The decreasing in the size of palladium crystallites lowered the temperature necessary to start of oxygen removal from the oxidized palladium phase. In the other words, the small crystallites of palladium oxide facilitate the oxidation of methane. The second peak of carbon dioxide, in the range of 370–385 °C, was also observed in the case of the TPR-CH₄ reduction of Pd/ZrO₂ [8] and Pd-M/HZSM-5 [36] catalysts and it was attributed [36] not directly to the palladium oxide reduction but to the product of side reactions (H₂O, CO) taking place over reduced palladium particles.

Water vapour (product of the reduction of PdO with hydrogen coming from methane) starts to be produced at the same temperatures as those of carbon dioxide formation, carbon monoxide begins to appear at about 300 °C. They are present in the effluent gas up to the end of our TPR experiments, i.e. up to 700 °C (those results are not shown in this paper).

The results of experiments on the oxygen isotope exchange (oxygen exchange in the higher-dispersed palladium catalyst occurs easier than in the catalyst with larger palladium crystallites) and those of the TPR with methane (small crystallites of palladium oxide facilitate the oxidation of methane) are important contributions to the knowledge of the properties of alumina-supported palladium catalysts with different dispersion of palladium phase.

Fig. 3A and B shows Pd 3d and O 1s spectra of the reduced alumina-supported palladium catalysts. Table 1 lists the binding energies (BEs) of palladium species located in the near-surface region of the catalysts, the surface composition, the ratio of surface concentrations of Pd and Al as well the as percentage of Pd and PdO in the palladium phase. The amount of palladium on the catalyst surface, inferred from the Pd/Al ratio (Table 1), increased from 0.217 for the sample Pd-13.0 to 0.555 for the sample Pd-4.6. This variation can be caused by larger coverage of the catalyst surface by palladium in the case of samples with smaller crystallites. As we can see in Fig. 3A, the binding energy tends to increase with the dispersion of palladium. The higher binding energies for palladium phase results from the presence of a higher amounts of PdO. The binding energies of Pd 3d indicate that palladium is present mostly

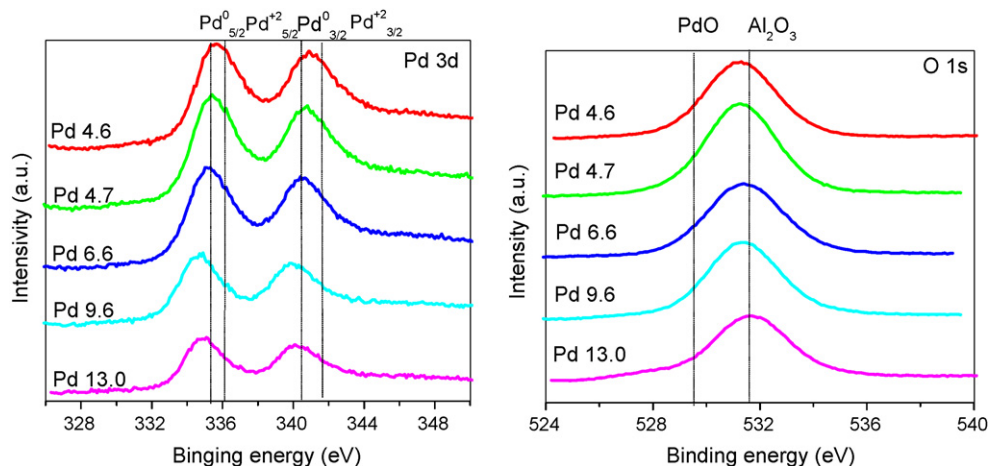


Fig. 3. XPS spectra for Pd 3d and O 1s of reduced palladium catalysts.

Table 1
Quantitative XPS data for reduced palladium catalysts

Catalyst	Mean size of palladium crystallites (nm)	Binding energy (eV)		Palladium phase surface composition (at.%)		Surface composition (at.%)			Surface Pd/Al ratio			
		Pd 3d _{5/2}	Pd 3d _{3/2}	Pd	PdO	Pd	Al	O	(at.%/at.%)	(w/w)		
Pd-4.6	4.6	335.6	337.6	340.8	342.8	85.1	14.9	4.7	33.7	61.6	0.140	0.555
Pd-4.7	4.7	335.4	337.6	340.6	342.6	88.3	11.7	4.2	34.5	61.3	0.121	0.479
Pd-6.6	6.6	335.2	337.4	340.5	342.7	90.2	9.8	4.0	33.6	62.4	0.118	0.469
Pd-9.6	9.6	334.6	336.6	340.0	342.1	98.0	2.0	2.2	37.1	60.7	0.057	0.229
Pd-13.0	13.0	334.8	336.8	340.2	342.2	91.6	8.4	2.0	36.7	61.3	0.055	0.217

as Pd⁰ (Pd 3d_{3/2} at 335.1 eV and Pd 3d_{5/2} at 340.5 eV), however, with a low fraction of PdO (Pd 3d_{3/2} at 336.0 eV and Pd 3d_{5/2} at 341.8 eV). As it is seen in Table 1, when the mean size of palladium crystallites is increased, the percentage of PdO decreased from 14.9 to 2.0 and that of Pd increased from 85.1 to 98.0. On the basis of the isotopic oxygen exchange, TPR-CH₄ and the XPS experiments we have concluded that oxygen from the support may change the oxidation state of palladium phase. The ratio of surface PdO and Pd amounts is higher in catalysts with smaller-sized palladium phase crystallites. We believe that it is also higher in the catalysts “working” in oxidation of methane and that the higher ratio of the surface PdO and Pd amounts changes also the number of the surface Pd–PdO sites that are thought as responsible for different activity of Pd(PdO)/Al₂O₃ catalysts in the methane oxidation reaction. The higher surface concentration of oxygen was suggested [9] to be favourable for activation of the C–H bond in the methane molecule.

As it was pointed out in Section 1, water vapour seriously affects the activity of palladium catalysts in the complete oxidation of methane. However, we have not found any report which elucidated the role of the palladium phase dispersion in determining the extent of that inhibiting effect of water vapour. Our catalysts enabled us to determine changes in the catalyst activity caused by the presence of water vapour, related only to the different dispersion of palladium phase, without any potential influence of different porosity of the catalyst support and different diffusion effects. This is another important contribution of our results to the knowledge of the flameless complete oxidation of methane over palladium-based catalysts.

The effect of water vapour on the activity of the supported palladium catalysts in the methane oxidation was investigated by varying the concentration of water in the feed stream from 0 to 20 vol.%. The results for the Pd-4.6 catalyst are shown in Fig. 4A. The complete oxidation of methane is achieved at 500 °C in

absence of water vapour. As water vapour concentration was increased the methane conversion curves shifts towards higher temperatures, hence the catalytic activity of the Pd-4.6 catalyst is deteriorated by water vapour. In spite of inhibiting influence of water vapour, even if its concentration was 20 vol.%, the total methane conversion over the Pd-4.6 catalyst was attained at the temperature lower than 650 °C (i.e., nitrogen oxides are not formed out of nitrogen and oxygen introduced with air).

In the case of the Pd-6.6 catalyst (Fig. 4B) the maximum conversion was achieved at 505 °C in the absence of water vapour, but the obtained maximum conversion level was only 96% at 690 °C when water vapour constituted 20 vol.% of the reaction mixture. At higher temperatures the activity of the Pd-6.6 catalyst decreased and then, above 860 °C, it again increased. According to Refs. [3–5,15], the observed minimum was explained by the complete decomposition of PdO to metallic palladium which is less active in methane oxidation. The presence of water vapour adsorbed on the surface of palladium phase facilitates disappearance of palladium oxide and, in consequence, probably facilitates disappearance of PdO–Pd sites. The next step of the increase of the methane conversion level may be attributed to the oxidation of methane not only over metallic palladium phase but also over Al₂O₃ support.

For the Pd-13.0 catalyst (Fig. 4C) the 100% of methane conversion in the absence of water vapour was achieved at 705 °C. In the case of water vapour presence (20 vol.%) the maximum of the methane conversion level was only 81% at 750 °C. At higher temperatures, as in the case of the Pd-6.6 catalyst, we observed a small catalyst deactivation.

The influence of water vapour on the oxidation of methane is different from catalyst to catalyst, depending on the dispersion of the palladium phase. The best catalysts for the complete oxidation of low-concentrated methane–air mixtures are those with small crystallites (<6.6 nm) of palladium. They may be successfully used

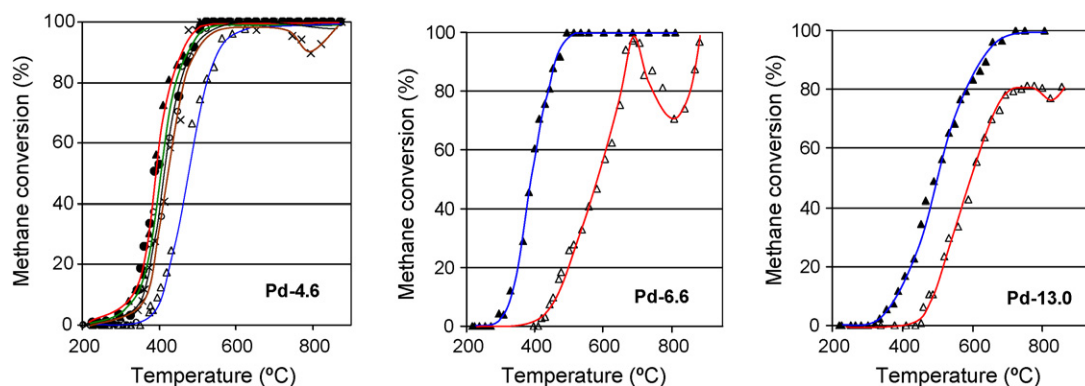


Fig. 4. Catalytic oxidation of methane over Pd-4.6, Pd-6.6, and Pd-13.0 catalysts (water vapour concentration in the reaction mixture: ((▲) 0 vol.%; (●) 5 vol.%; (○) 10 vol.%; (×) 15 vol.%; (△) 20 vol.%).

for mitigation of methane emission from humid post-ventilation air from coal mines and, after increasing of the methane concentration to 1–2 vol.%, for its utilization for the energy production. The increased concentration of water vapour (as the reaction product) along the catalyst bed will be negligible and the 100% conversion of methane will be achieved at the temperatures below 650 °C. The lowest dependence of catalysts with small crystallites of the palladium phase on the water vapour inhibiting influence is consistent with suggestions of Ciuparu et al. [37] that a high oxygen mobility in the catalyst accelerates desorption of hydroxyls, leading to only moderate inhibition of the activity of such catalysts by water.

4. Conclusions

The small crystallites of palladium phase in the Pd/Al₂O₃ catalyst decrease temperatures necessary to ignite (start) the methane oxidation reaction and to achieve complete conversion of methane. Our studies (the isotopic exchange of oxygen between the catalyst and the gas phase, the temperature-programmed reduction with methane and the X-ray photoelectron spectroscopy) suggest that it can result from a higher number of the Pd–PdO sites present on the catalysts with small palladium crystallites. The inhibiting effect of water vapour present in the reaction mixture increases with lower dispersion of palladium phase as well as with the water concentration in the feed. The larger palladium crystallites are more significantly affected by the presence of water. It may be concluded that the water vapour blocks the Pd–PdO active sites.

The catalytic oxidation is an environmental benign method for utilization of various methane-poor gas mixtures, including humid post-ventilation air of coal mines. The alumina-supported palladium catalysts with small crystallites (<6.6 nm) of palladium can be successfully used for mitigation of the emission of methane from coal mine post-ventilation air and, after increasing of the methane concentration to 1–2 vol.%, for its utilization for the energy production. In the case of such catalysts even a high concentration of water vapour, expected as the reaction product at the end of the catalyst bed, has the least negative influence on the catalyst activity and it will not interfere with obtaining of the 100% conversion of methane below 650 °C.

References

- [1] US Environmental Protection Agency Assessment of the Worldwide Market Potential for Oxidizing Coal Mine Ventilation Air Methane, EPA 430R03002, July (2003), www.epa.gov/coalbed/pdf/ventilation_air_methane.pdf.
- [2] D. Ciuparu, M.R. Lyubovsky, E. Altman, L.D. Pfefferle, A. Datye, *Catal. Rev.* 44 (2002) 593, and references cited therein.
- [3] P. Gelin, M. Primet, *Appl. Catal. B* 39 (2002) 1, and references cited therein.
- [4] T.V. Choudhary, S. Banerjee, V.R. Choudhary, *Appl. Catal. A* 234 (2002) 1, and references cited therein.
- [5] G. Centi, *J. Mol. Catal. A* 173 (2001) 287, and references cited therein.
- [6] J.H. Lee, D.L. Trimm, *Fuel Process. Technol.* 42 (1995) 339, and references cited therein.
- [7] R.F. Hicks, H. Qi, M.L. Young, R.G. Lee, *J. Catal.* 122 (1990) 295.
- [8] Ch.A. Müller, M. Maciejewski, R.A. Koeppl, A. Baiker, *J. Catal.* 166 (1997) 36.
- [9] K.I. Fujimoto, F.H. Ribeiro, M.A. Borja, E. Iglesia, *J. Catal.* 179 (1998) 431.
- [10] D. Ciuparu, L. Pfefferle, *Appl. Catal. A* 209 (2001) 415.
- [11] D. Ciuparu, E. Altman, L. Pfefferle, *J. Catal.* 203 (2001) 64.
- [12] W. Lin, Y.X. Zhu, N.Z. Wu, Y.C. Xie, I. Murwani, E. Kemnitz, *Appl. Catal. B* 50 (2004) 59.
- [13] F.H. Ribeiro, M. Chow, R.A. Dalla Betta, *J. Catal.* 146 (1994) 537.
- [14] R. Kikuchi, S. Madea, K. Sasaki, S. Wennerström, K. Eguchi, *Appl. Catal. A* 232 (2002) 23.
- [15] T.V. Choudhary, S. Banerjee, V.R. Choudhary, *Catal. Commun.* 6 (2005) 97.
- [16] H. Yoshida, T. Nakajima, Y. Yazawa, T. Hattori, *Appl. Catal. B* 71 (2007) 70.
- [17] J.C. van Giezen, F.R. van den Berg, J.L. Kleinen, A.J. van Dillen, J.W. Geus, *Catal. Today* 47 (1999) 287.
- [18] W. Ibbashi, G. Groppi, P. Forzatti, *Catal. Today* 83 (2003) 115.
- [19] P. Araya, S. Guerrero, J. Robertson, F.J. Gracia, *Appl. Catal. A* 283 (2005) 225.
- [20] R. Burch, F.J. Urbano, P.K. Loader, *Appl. Catal. A* 123 (1995) 173.
- [21] R. Burch, D.J. Crittle, M.J. Hayes, *Catal. Today* 47 (1999) 229.
- [22] K. Persson, L.D. Pfefferle, W. Schwartz, A. Ersson, S.G. Järås, *Appl. Catal. B* 74 (2007) 242.
- [23] P. Hurtado, S. Ordonez, H. Sastre, F.V. Diez, *Appl. Catal. B* 51 (2004) 229.
- [24] P. Gelin, L. Urfels, M. Primet, E. Tena, *Catal. Today* 83 (2003) 45.
- [25] P. Hurtado, S. Ordonez, H. Sastre, F.V. Diez, *Appl. Catal. B* 47 (2004) 85.
- [26] K. Narui, H. Yata, K. Furata, A. Nishida, Y. Kohtoku, T. Matsuzaki, *Appl. Catal. A* 179 (1999) 165.
- [27] D. Ciuparu, N. Katsikis, L. Pfefferle, *Appl. Catal. A* 216 (2001) 209.
- [28] G. Groppi, *Catal. Today* 77 (2003) 335.
- [29] S. Eriksson, M. Boutonnet, S. Järås, *Appl. Catal. A* 312 (2006) 95.
- [30] K. Okumura, E. Shinohara, M. Niwa, *Catal. Today* 117 (2006) 577.
- [31] J.A.C. Ruiz, M.A. Fraga, H.O. Pastore, *Appl. Catal. B* 76 (2007) 115.
- [32] A.K. Datye, J. Bravo, T.R. Nelson, P. Atanasova, M. Lyubovsky, L. Pfefferle, *Appl. Catal. A* 199 (2000) 179.
- [33] J. Barcicki, D. Nazimek, W. Grzegorzczak, T. Borowiecki, R. Frak, M. Pielach, *React. Kinet. Catal. Lett.* 17 (1981) 169.
- [34] A. Machocki, B. Stasinska, W. Gac, in: P. Forzatti, G. Groppi, P. Ciambelli, D. Sannino (Eds.), *Catalytic Combustion*, vol. 2, Polipress, Milano, 2005, p. 155.
- [35] A. Machocki, B. Stasinska, W. Gac, *Pol. J. Chem. Technol.* 8 (2006) 93.
- [36] C. Shi, L. Yang, Z. Wang, X. He, J. Cai, G. Li, X. Wang, *Appl. Catal. A* 243 (2003) 379.
- [37] D. Ciuparu, E. Perkins, L. Pfefferle, *Appl. Catal. A* 263 (2004) 145.